Combustion Stability Characteristics of the Model Chamber with Various Configurations of Triplet Impinging-Jet Injectors

Chae Hoon Sohn*
Department of Aerospace Engineering, Chosun University, Gwangju 501-759, Korea
Woo-Seok Seol
Rocket Engine Department, Korea Aerospace Research Institute, P.O. Box 113, Yusung, Daejeon 305-600, Korea
Alexander A. Shibanov
Research Institute of Chemical Machine Building (NIICHIMMASH), Sergiev Posad, Russia

Combustion stability characteristics in actual full-scale combustion chamber of a rocket engine are investigated by experimental tests with the model (sub-scale) chamber. The present hot-fire tests adopt the combustion chamber with three configurations of triplet impinging-jet injectors such as F-O-O-F, F-O-F, and O-F-O configurations. Combustion stability boundaries are obtained and presented by the parameters of combustion-chamber pressure and mixture (oxidizer/fuel) ratio. From the experimental tests, two instability regions are observed and the pressure oscillations have the similar patterns irrespective of injector configuration. But, the O-F-O injector configuration shows broader upper-instability region than the other configurations. To verify the instability mechanism for the lower and upper instability regions, air-purge acoustic test is conducted and the photograph of the flames is taken. As a result, it is found that the pressure oscillations in the two regions can be characterized by the first impinging point of hydraulic jets and pre-blowout combustion, respectively.

Key Words : Combustion Stability, Stability Boundary, Hot-Fire Test, Model Chamber, Triplet Impinging-Jet Injectors

1. Introduction

High-frequency combustion instability is the phenomenon that pressure oscillations are amplified through in-phase heat addition/extraction from combustion. It is often called acoustic instability, which has long gained significant interest in propulsion and power systems. It has been reported that it may lead to an intense pressure fluctuation as well as excessive heat transfer to combustor wall in combustion systems such as solid and liquid propellant rocket engines, ramjets, turbojet thrust augmentors, utility boilers, and furnaces (Harrje and Reardon, 1972 ; McManus et al., 1993 ; Culick and Yang, 1995). For a long time, it has caused common problems in the course of combustion-chamber development, especially, rocket-combustor development.

Due to the destructive effect of strong pressure oscillation, combustion stability should be considered carefully by engine designers. In this regard, the impact of various candidate injectors on stabilities is to be examined for injector screening at the initial stage of combustor development, and thereby the suitable injector configuration will

* Corresponding Author,
E-mail : chsohn@chosun.ac.kr
TEL : +82-62-230-7123; **FAX** : +82-62-230-7123
Department of Aerospace Engineering, Chosun University, Gwangju 501-759, Korea. (Manuscript **Received** October 12, 2005; **Revised** March 16, 2006)

be selected. For this purpose, it is the best and most reliable method to conduct experimental test using full-scale combustion chambers to which candidate injectors are mounted. But, it is rather exhaustive method in both viewpoints of cost and time. As one of more cost-effective methods, the previous works (Dexter et al., 1995 ; Sohn et al., 2004) have proposed the methodologies of the hot- fire injector test adopting the model (sub-scale) chamber but with actual injectors. And, Sohn et al.(2005) conducted the hot-fire injector test based on the methodologies, obtained combustion stability boundaries and suggested the instability mechanisms of F(fuel)-O(oxidizer)-O-F split-triplet impinging-jet injectors.

In the rocket combustor, there can be adopted various configurations of triplet impinging-jet injectors. Each configuration may show different stability characteristics and thereby, has its own stability boundary. Accordingly, the present study adopts three principal configurations of the triplet jet injectors such as F-O-O-F, F-O-F, and O-F-O and provides stability boundary of each configuration and information on instability mechanism.

2. Experimental Methods

2.1 Full-scale chamber and injector

In this study, the same full-scale combustion chamber as in the previous study (Sohn et al., 2005) is adopted. The chamber employs a liquid-liquid scheme injector with the following propellants ; hydrocarbon fuel (kerosene) and cryogenic oxidizer (liquid oxygen). Schematic diagrams and basic geometrical dimensions of the combustion chamber and injector can be found in the literature (Sohn et al., 2005). For the design operating condition, chamber pressure, P_{ch} and mixture ratio, K_m are 1.4 MPa and 2.34, respectively. And the other major operating parameters of the combustion chamber can be found in table 1 of the previous paper (Sohn et al., 2004).

Injector head is fitted with identical bi-propellant injectors in the number of n_{in}=216 pieces arranged equidistantly on the injector faceplate. The basic injector configuration, i.e., F-O-O-F injector has two orifices for oxidizer injection with the diameter (d_O) of 2.2 mm and two orifices for fuel supply with d_F=1.6 mm, which is illustrated in Fig. 1(a). At the impinging angle of 60°, two fuel jets are injected, arranged to the left and to the right of each oxidizer jet, respectively. Main hydrodynamic parameters of the injector also can be found in table 1 of the previous paper (Sohn et al., 2004). The other injector configurations, F-O-F and O-F-O are shown in Fig. 1(b)

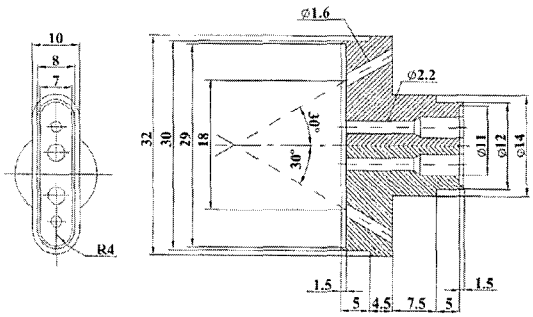

(a) F-O-O-F injector configuration

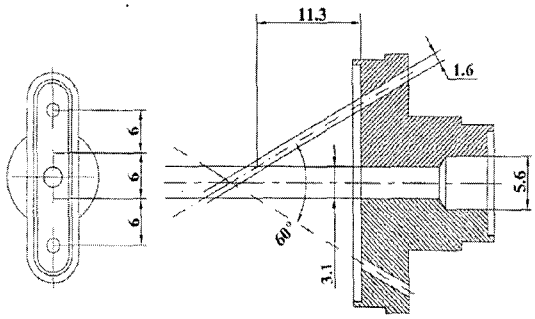

(b) F-O-F injector configuration

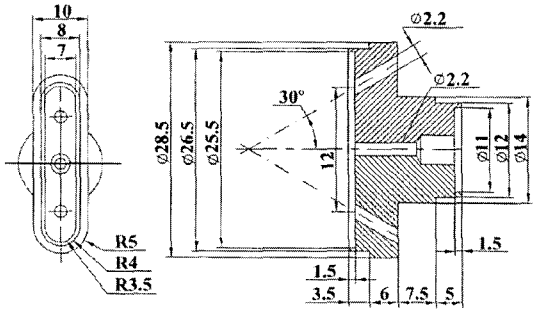

(c) O-F-O injector configuration

Fig. 1 Schematic diagram of the configurations of bi-propellant impinging jet injectors : (a) F-O-O-F, (b) F-O-F, and (c) O-F-O configurations (unit : mm)

and 1(c), respectively.

2.2 Model-test apparatus and test procedures for hot-fire tests

Schematic diagram of the firing-test model setup was shown in the previous work (Sohn et al., 2005). The same apparatus is used here, and the five-injector unit is made replaceable to test three injector configurations. The combustion chamber operates at atmospheric pressure and can move freely on the injector-faceplate simulator to excite the pressure oscillations of the tangential acoustic modes. Pure gaseous oxygen is supplied through the oxidizer feeding line and the fuel line supplies gaseous methane-propane mixture at room temperature.

The model-test apparatus is used to determine the boundaries of the regions of acoustic oscillations excited at the specific flow rates of propellants. Accordingly, pressure pulsations from the combustion field in the model chamber are measured with an acoustic probe, which is inserted into the hole made on the chamber wall near the faceplate of the model injector head. The signal from the transducer is amplified by the broad-band amplifier, recorded by personal computer, and also sent to visual instruments, i.e., oscilloscope, digital voltmeter, and spectrum analyzer.

Details on measurement methods and test procedures can be found in the literature (Sohn et al., 2005). Boundaries separating stable and unstable operating conditions are usually not so clear. To catch smooth onset of unstable combustion, the operating condition is changed minutely. When determining self-excitation boundaries for the injectors, the ranges of fuel and oxidizer volumetric flow rates simulates the actual volumetric flow rates corresponding to the design operating regime of the combustion chamber. And with oxidizer and fuel density predetermined, the range of propellant mass flow rate can be determined. To cover the wide range of operating conditions including the design point, the wide ranges of mass flow rates are adopted with each injector configuration.

In the course of signal processing, the data of oscillation frequency f, amplitude A, and damping factor, η (Laudien et al., 1995) for ten major spectral maxima are printed in tables and spectrograms are printed out in each regime. Smaller damping factor indicates stronger acoustic resonance, i.e., stronger pressure oscillation. Model-test data are scaled-up to actual operating conditions by the procedures described in the previous work (Sohn et al., 2004).

2.3 Model chamber

The method to select the geometry of model combustion chamber acting as an acoustic resonator at a variety of oscillating natural frequencies, f_{ch} has been described in detail in Sohn et al.'s work (2004). Based on the method, the geometric dimensions of the model chamber are chosen to provide the same natural frequencies in model chamber as those in actual chamber. The diameter and the length of the model chamber were calculated as $D_{ch,m}=170\sim180$ mm and $L_{ch,m}=240\sim260$ mm, respectively. With these dimensions selected, the resonant frequencies of the two principal transverse oscillatory modes, 1T (the 1st tangential mode) and 1T1L (the combined acoustic mode of the 1st tangential and the 1st longitudinal modes) are estimated to be $f_{1T}=$ 1561 Hz and $f_{1T1L}\cong1923$ Hz, respectively.

2.4 Model-test apparatus for acoustic tests

To examine the mechanism of instability triggering hydraulically, air-purge acoustic tests are conducted as well, where air is injected through both fuel and oxidizer orifices. The model setup is presented schematically in Fig. 2. A honeycomb is installed inside the model chamber to simulate a combustion zone and it has the form of the circular beam with the short length of 15 mm and the variable diameter, d_{cz}. The adjustable distance from the mixing element exit to the honeycomb surface, l_{cz} simulates the characteristic length of a combustion zone.

Mixing element, i.e., five-injector unit is installed flush with the plate. Air is supplied to the mixing element through the manifold to fuel and oxidizer feed cavities separately. A model chamber of diameter, D_{ch} and length L_{ch} with a microphone attached to the wall is installed on the

plate. Signal measured by the microphone is fed to the oscillograph and spectrum analyzer. Oscillation excitation mode is identified by the acoustic probe, which sends a signal to the second channel of the oscillograph.

Air at the pressure P_{inl} passes the metering orifice and enters the supply lines of the mixing element. Hand valves can cut off one of two feed cavities, and also regulate flow-rate ratio of oxidizer to fuel. Pilot pressure probe (0.8 mm tube with the hole of 0.5 mm diameter) and U-shaped manometer senses dynamic pressure of oxidizer and fuel jets as well as the joined flow upon impingement of the jets. Mach number M and flow velocity U are calculated from the measured dynamic pressure on the axis. Frequencies, f and oscillation amplitude, A are obtained by the spectrum analyzer for each oscillation mode and damping factors are calculated.

Air-purge test procedures are as follows. At first, we set a minimum air flow rate to the fuel manifold. After that, the air flow rate through the oxidizer manifold is raised gradually by a certain step. Operating conditions and pressure oscillations in the model chamber at each step are recorded. And then, a higher constant air flow rate through the fuel manifold is set and all operations are repeated.

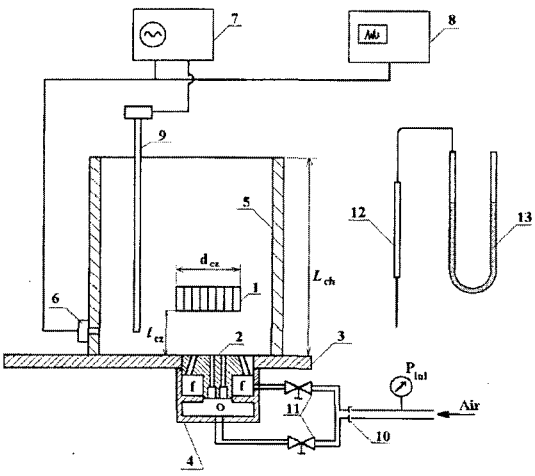

1 : honeycomb, 2 : mixing element, 3 : plate, 4 : manifold, 5 : chamber, 6 : microphone, 7 : oscillograph, 8 : spectrum analyzer, 9 : acoustic probe, 10 : metering orifice, 11 : hand valves, 12 : pilot pressure probe, 13 : liquid manometer

Fig. 2 Schematic diagram of experimental apparatus for air-purge acoustic test

3. Results and Discussions

3.1 Stability boundaries

First, the instability-region boundaries of the chamber with F-O-O-F injectors are measured and shown in Fig. 3 on the coordinate plane of chamber pressure, P_{ch} vs. mixture ratio, K_m. Chamber pressure is calculated using total mass flow rate, the characteristic velocity, and the nozzle throat area as described in the previous work (Sohn et al., 2004 ; Sutton, 2001). In Fig. 3, the rectangular region, of which center indicates the design operating point, shows possible operating conditions of the actual rocket combustor during the flight with sufficient margin. It is often called operating window or range. From this figure, it can be seen that combustion process established by the present injectors features two principal unstable regions ; lower and upper ones. The lower region of high-frequency oscillations at the frequency of $f_{1T1L}=1850\pm150$ Hz (denoted by the region, HFO-I) is located on the left of the actual operating range. The stability margin, $\bar{R}$ is defined as

$$\bar{R}=\left[\left(\frac{\Delta P_{ch}}{P_{ch,des}}\right)^2+\left(\frac{\Delta K_m}{K_{m,des}}\right)^2\right]^{0.5} \quad (1)$$

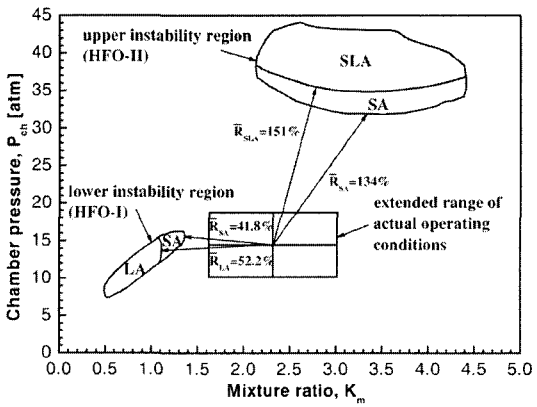

Fig. 3 Stability boundaries and margins plotted on the coordinate of chamber pressure vs. mixture ratio in the chamber with F-O-O-F injector configuration

where $\Delta P_{ch}=P_{ch}-P_{ch,des}$, $\Delta K_m=K_m-K_{m,des}$, and the subscript, *des* denotes design operating condition. The stability margin toward two regions ranges from 41.8~151%. The lower instability region is relatively close to the operating window, whereas the upper instability region is far from it.

The dynamic characteristics of pressure oscillation in two regions were discussed in detail in the previous work (Sohn et al., 2005) and omitted here. In Fig. 3, SA, LA, and SLA indicate the oscillations with small, large, and super-large amplitudes, respectively. As a rule, the amplitude of small-amplitude oscillation is about 3~4 times higher than the noise level, where large amplitude is more than 10 times as high as the noise level. The oscillation with super-large amplitude shows the peculiar pattern of frequency spectrum as shown in Fig. 7 of the previous paper (Sohn et al., 2005) ; multiple peaks corresponding to harmonics of the fundamental peak.

Next, the instability-region boundaries of the chamber with F-O-F injectors are measured and shown in Fig. 4. The location and shape of the instability region is similar to that in the chamber with F-O-O-F injectors. The stability margins are increased toward both instability regions and especially, increased appreciably toward the upper instability region. It is found that the dynamic behaviors of the flames in each instability region are fundamentally same as those in case of F-O-O-F injectors. As discussed in the previous study (Sohn et al., 2005), the instability triggering in the lower instability region is related with the first impinging point of fuel and oxidizer jets. The F-O-F configuration also has the first impinging point of $O(10\,\text{mm})$ away from the injector faceplate as shown in Fig. 1(b) and thereby, the similar behaviors to in the F-O-O-F configuration are observed. On the other hand, it was predicted that the instability in the upper region is closely related with pre-blowout combustion. The area of the upper region is smaller than that in the F-O-O-F configuration with respect to both pressure and mixture ratio. While the F-O-O-F configuration has the second impinging point, the F-O-F configuration does not have. The existence of the upper instability region indicates that two configurations have the fundamentally same behaviors of flames near blowout condition irrespective of the second impinging. But, from the reduced unstable area in F-O-F configuration without the second impinging point, the second impinging of jets affect combustion characteristics, leading to a wider operating range of pre-blowout condition.

The instability-region boundaries of the chamber with O-F-O injectors are measured and shown in Fig. 5. The location and shape of the instability region is similar to that in the cham-

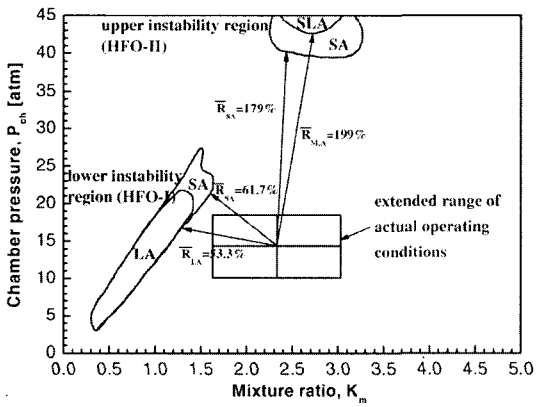

Fig. 4 Stability boundaries and margins plotted on the coordinate of chamber pressure vs. mixture ratio in the chamber with F-O-F injector configuration

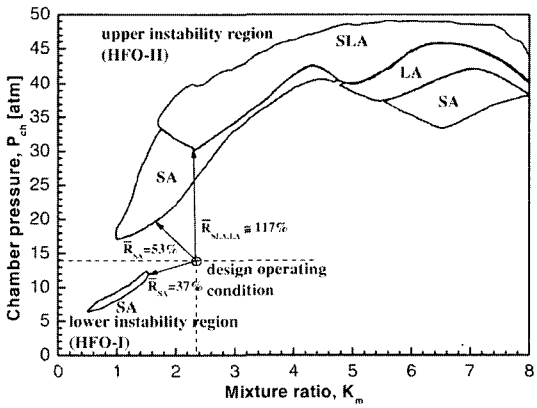

Fig. 5 Stability boundaries and margins plotted on the coordinate of chamber pressure vs. mixture ratio in the chamber with O-F-O injector configuration

bers with F-O-O-F and F-O-F injectors. But, stability margins are reduced appreciably. Even without the second impinging point, the upper instability region is observed and especially, the area of the region is greatly enlarged toward a higher range of mixture ratio. The O-F-O configuration has the first impinging point with O (10 mm), but the propellant-jets arrangement in space is different from the other two configurations. This makes different mixing pattern from the F-O-(O-)F configuration. In the O-F-O configuration, oxidizer streams surround fuel jet and some part of the oxidizer is not reacted completely with fuel. From the standpoint of chemical reaction, this causes fuel-rich condition and local equivalence ratio deviates farther away from unity because overall equivalence ratio of the chamber for design operating condition is less than unity.

From the above experimental data, it is found that instability triggering in the lower instability region results from the hydraulic jet-impinging and in the upper region, it is mostly related with the combustion characteristics. These points are discussed in more detail in the following sections.

3.2 Air-purge acoustic tests

By supplying air to oxidizer and fuel manifolds of the model five-element injector head, we can simulate mixing processes of streams flowing from oxidizer and fuel orifices under cold-flow conditions without chemical reaction. Further, it will be interesting to correlate acoustic-test data with combustion-acoustic stability from hot-fire tests of the model injector head.

During the air-purge test, we intended (as in the course of hot-fire tests) to determine self-oscillation boundaries. However, the experiments have shown that determination of these boundaries was hindered by less distinct momentum of self-oscillation excitation. Therefore, based on the fact that unstable operation with small-amplitude oscillation differs from stable operation mainly in oscillation regularity characterized by the damping factor, we approached the acoustic-test procedure as close as possible to hot-fire test procedure to determine stability boundaries.

The honeycomb, which is adopted to amplify the oscillation by a certain section of the combustion zone (mixing zone), is installed away from the injector faceplate to a distance of l_{cz}. The honeycomb is placed at a distance of $l=10$ mm from the injector faceplate. As an example, with the F-O-O-F configuration, the measured damping factors are shown as a function of q at the fuel flow rate of $\dot{m}_F=1.01$ g/s in Fig. 6, where q is defined by velocity and density ratios in the form

$$q=\frac{U_O}{U_F}\left(\frac{\rho_O}{\rho_F}\right)^{0.5} \tag{2}$$

In Fig. 6, the operating conditions with local minimum of damping factor with respect to q correspond to the stability boundary. From the

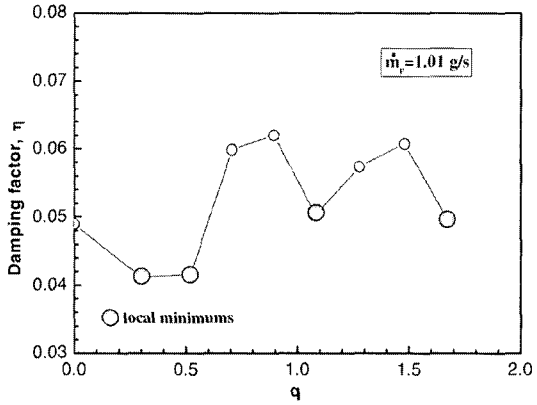

Fig. 6 Damping factor as a function of q in air-purge acoustic test with F-O-O-F injector configuration ($q=U_O/U_F\sqrt{\rho_O/\rho_F}$)

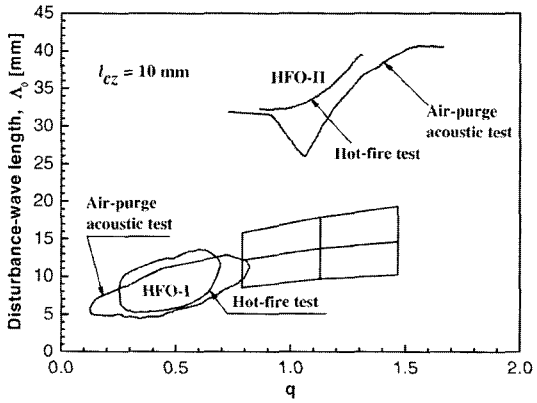

Fig. 7 Stability boundaries plotted on the coordinate of disturbance-wave length, Λ_O vs. q

data over the wide ranges of $\dot{m}_F$ and $\dot{m}_O$, stability boundaries are obtained and shown in Fig. 7 on the coordinate of Λ_O and q, where disturbance-wave length, $\Lambda_O \equiv U_O/f_{ch}$. It can be seen that lower instability boundaries determined by hot-fire and acoustic tests are fairly close to each other. But, the upper instability boundary is predicted relatively poorly. This point indicates that the lower instability boundary is closely related with the hydraulic jet-impinging point.

3.3 Flame behaviors in the O-F-O injector configuration

In the preceding section, it is shown that instability regions in the O-F-O configuration have the similar pattern to in the F-O-O-F configuration, but broader upper instability region. As aforementioned, pressure oscillation with super-large amplitude is observed in the upper region and it is related with pre-blowout combustion.

Observation of the injector flame produced by a five-element model injector with the O-F-O configuration shows that the flame is blue at the stable operation mode being close to the stability boundary, which indicates an intense mixing of oxidizer with fuel and a violent combustion process. But as soon as SLA (super-large amplitude) oscillation occurs, the change in both flame color and pattern is noted. The flame becomes darker and exhibits yellow strips, which implies inadequate combustion of the fuel. Under actual operating conditions, this effect may result in decreased combustion efficiency, which has been usually observed during excitation of high-frequency oscillation of SLA type in an actual combustion chamber (Sohn et al., 2003).

From instability boundaries presented on the coordinate of Λ_O and q, which is not shown here, it is found that the lower instability region with SA (small-amplitude) oscillation at a frequency $f_{1T1L}=1550\sim1750$ Hz is caused by unsteady nature of the first impinging point of oxidizer and fuel spray fans. This conclusion is based on the fact that the distance of the impingement point from the injector faceplate ($\sim$14 mm) is close to the parameter, Λ_O for unsteady operating conditions in this region ; $\Lambda_O=9\sim14$ mm.

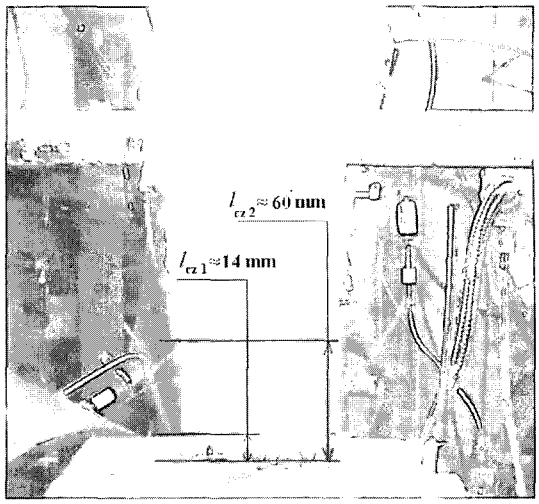

Fig. 8 Photograph of the flames formed for one operating condition in upper instability region ($U_O=56$ m/s, $U_F=62.5$ m/s, $q=1.12$, and $K_m=2.81$)

Figure 8 shows the photograph of injector flame for one operating condition of $U_O=56$ m/s, $U_F=62.5$ m/s, $q=1.12$, and $K_m=2.81$ in the upper instability region. Two characteristic longitudinal lengths of the combustion zone, $l_{cz,1}\cong14$ mm and $l_{cz,2}\cong60$ mm are presented, which denote the maximum luminant point and the upper boundary of intensive flame, respectively. The length, $l_{cz,1}\cong14$ mm corresponds to the calculated distance from the injector faceplate to the first impingement point of oxidizer and fuel streams. The length, $l_{cz,2}\cong60$ mm can be construed as a characteristic length of the combustion zone, where clouds of unburned mixture burn out violently. The length, $l_{cz,2}$ is close to the parameter of Λ_O for SLA oscillation, which indicates the instability triggering in the upper instability region is more related with combustion characteristics of pre-blowout rather than hydraulic jet-impinging.

4. Concluding Remarks

Combustion stability characteristics in actual full-scale combustion chamber of a rocket engine have been investigated by experimental tests with the model (sub-scale) chamber with various configurations of triplet impinging-jet injectors such

as F-O-O-F, F-O-F, and O-F-O configurations. Combustion stability boundaries have been obtained and presented by the parameters of combustion-chamber pressure and mixture (oxidizer/fuel) ratio.

From the experimental tests, two instability regions have been observed and the pressure oscillations have had the similar patterns irrespective of injector configuration. But, the O-F-O injector configuration has shown broader upper-instability region than the other configurations. To verify the instability mechanism for the lower and upper instability regions, air-purge acoustic test has been conducted and the photographs of the flames are taken. As a result, it has been found that the pressure oscillations in the lower instability region can be characterized hydraulically by the first jet-impinging point and those in the upper instability region are closely related with pre-blowout combustion near extinction condition of flames. From the standpoint of pressure oscillation with super-large amplitude, the O-F-O injector configuration has worse stability than the other configurations because it causes locally low equivalence ratio. On the other hand, the F-O-F injector configuration is recommended as relatively better injector configuration.

References

Culick, F. E. C. and Yang, V., 1995, in *Liquid Rocket Engine Combustion Instability* (Edited by Yang, V. and Anderson, W. E.), *Progress in Astronautics and Aeronautics*, Vol. 169, AIAA, Washington DC, pp. 3～38.

Dexter, C. E., Fisher, M. F., Hulka, J. R., Denisov, K. P., Shibanov, A. A., and Agarkov, A. F., 1995, "Scaling Techniques in Liquid Rocket Engine Combustion Devices Testing," *The Second International Symposium on Liquid Rocket Engines*, Paris.

Harrje, D. J. and Reardon, F. H.(eds.), 1972, *Liquid Propellant Rocket Combustion Instability*, NASA SP-194.

Laudien, E., Pongratz, R., Pierro, R. and Preclik, D., 1995, in *Liquid Rocket Engine Combustion Instability* (Edited by Yang, V. and Anderson, W. E.), *Progress in Astronautics and Aeronautics*, Vol. 169, AIAA, Washington DC, pp. 377～399.

McManus, K. R., Poinsot, T. and Candel, S. M., 1993, "A Review of Active Control of Combustion Instabilities," *Progress in Energy and Combustion Science*, Vol. 19, pp. 1～29.

Sohn, C. H., Seol, W. -S., Lee, S. Y., Kim, Y. -M. and Lee, D. S., 2003, "Application of Combustion Stabilization Devices to Liquid Rocket Engine," *Journal of The Korean Society for Aeronautical and Space Sciences* (in Korea), Vol. 31, No. 6, pp. 79～87.

Sohn, C. H., Seol, W. -S., Shibanov, A. A. and Pikalov, V. P., 2004, "On the Method for Hot-Fire Modeling of High-Frequency Combustion Instability in Liquid Rocket Engines," *KSME International Journal*, Vol. 18, No. 6, pp. 1010～1018.

Sohn, C. H., Seol, W. -S., Shibanov, A. A. and Pikalov, V. P., 2005, "Hot-Fire Injector Test for Determination of Combustion Stability Boundaries Using Model Chamber," *Journal of Mechanical Science and Technology*, Vol. 19, No. 9, pp. 1821～1832.

Sutton, G. P., 2001, *Rocket Propulsion Elements*, 7th Ed., John Wiley & Sons, Inc., New York.